Title

A sensitive fluorometric bio-barcodes immunoassay for detection of triazophos residue in agricultural products and water samples by iterative cycles of DNA-RNA hybridization and dissociation of fluorophores by Ribonuclease H

Authors

Zhang, Xiuyuan
Du, Pengfei
Cui, Xueyan
et al.

Publication Date

2020-05-01

DOI

10.1016/j.scitotenv.2020.137268

Peer reviewed

HHS Public Access

Author manuscript

Sci Total Environ. Author manuscript; available in PMC 2021 May 15.

Published in final edited form as:

Sci Total Environ. 2020 May 15; 717: 137268. doi:10.1016/j.scitotenv.2020.137268.

A sensitive fluorometric bio-barcodes immunoassay for detection of triazophos residue in agricultural products and water samples by iterative cycles of DNA-RNA hybridization and dissociation of fluorophores by Ribonuclease H

Xiuyuan Zhang[a,b], **Pengfei Du**[b], **Xueyan Cui**[b], **Ge Chen**[b], **Yuanshang Wang**[b], **Yudan Zhang**[b], **A. M. Abd El-Aty**[c,d], **Ahmet Hacimüftüoğlu**[d], **Jing Wang**[b], **Hongjun He**[a,*], **Maojun Jin**[b,e,*], **Bruce Hammock**[e]

[a]College of Life Sciences, YanTai University, Yantai, 264005, China

[b]Key Laboratory of Agro-product Quality and Food Safety, Institute of Quality Standard &Testing Technology for Agro-Products, Chinses Academy of Agricultural Science, Beijing, 100081, China

[c]Department of Pharmacology, Faculty of Veterinary Medicine, Cairo University, 12211 Giza, Egypt

[d]Department of Medical Pharmacology, Medical Faculty, Ataturk University, 25240-Erzurum, Turkey

[e]Department of Entomology & Nematology and the UC Davis Comprehensive Cancer Center, Davis, CA 95616, USA

Abstract

Although the toxicity of triazophos is high and it has been pulled from the market in many countries; it is still widely used and frequently detected in agricultural products. While conventional analyses have been routinely used for the quantification and monitoring of triazophos residues, those for detecting low residual levels are deemed necessary. Therefore, we developed a novel and sensitive fluorometric signal amplification immunoassay employing bio-barcodes for the quantitative analysis of triazophos residues in foodstuffs and surface water. Herein, monoclonal antibodies (mAbs) attached to gold nanoparticles (AuNPs) were coated with DNA oligonucleotides (used as a signal generator), and a complementary fluorogenic RNA was used for signal amplification. The system generated detection signals through DNA-RNA hybridization and subsequent dissociation of fluorophores by Ribonuclease H (RNase H). It has to be noted that RNase H can only disintegrate the RNA in DNA-RNA duplex, but not cleave single or double-stranded DNA. Hence, with iterative cycles of DNA-RNA hybridization, sufficient strong signal was obtained for reliable detection of residues. Furthermore, this method enables quantitative detection of triazophos residues through fluorescence intensity measurements. The competitive immunoassay shows a wide linear range of 0.01–100 ng/mL with a limit of detection (LOD) of

*Corresponding authors: Hongjun He, hemiles@163.com; Tel.:+86-156-6802-8169 Maojun Jin, jinmaojun@caas.cn, Tel.: +86-10-8210-6570.

Conflicts of interest

The authors declare no competing financial interest.

0.0032 ng/mL. The assay substantially meets the demand for the low residue detection of triazophos residues in agricultural products and water samples. Accuracy (expressed as spiked recovery %) and coefficient of variation (CV) were ranged from 73.4% to 116% and 7.04% to 17.4%, respectively. The proposed bio-barcodes immunoassay has the advantages of being stable, reproducible, and reliable for residue detection. In sum, the present study provides a novel approach for detection of small molecules in various sample matrices.

Keywords

Competitive immunoassay; Amplification strategy; Organophosphate pesticides; Fluorescence; Matrix effect

1. Introduction

Triazophos, an organophosphate pesticide with a broad spectrum and moderate toxicity, is recognized as an important insecticide on a variety of agricultural crops in China (Guo et al., 2018). It is widely used to control insects, acarids, and some nematodes in fruit trees, cotton, and grain to increase yield (Liu et al., 2018). In addition, with the prohibition of using highly toxic and residual organophosphates, such as methyl parathion, methamidophos, and parathion on crops, there has been an explosion in the use of triazophos during recent years (Tang and You, 2012). However, one can never neglect the fact that triazophos irreversibly inhibits acetylcholinesterase and causes the accumulation of acetylcholine, which has harmful effects on nervous systems (Singh et al., 2018). Additionally, residual triazophos was found in surface water, fruits, and vegetables, owing to its relative stability and low speed of degradation. The resulting exposures pose a significant risk to human health (Bhanot and Sangha, 2018).

Conventional pesticide residue detection methods, including gas chromatography (GC) (Hayward et al., 2015), high-performance liquid chromatography (HPLC), and gas or liquid chromatography combined with mass spectrometry (GC-MS/LC-MS) (Casado et al., 2019; Rai et al., 2016), are sensitive and accurate, however, they require long analysis times and sophisticated equipment (Taha and Gadalla, 2017). Recently, immunoassays such as a colorimetric enzyme-linked immunosorbent assay (ELISA) (Li et al., 2014), chemiluminescence immunoassay (Wang et al., 2013) and fluoroimmunoassay (Lu et al., 2017) have attracted increasing attention for detection of pesticide residues, due to their rapid and simple approaches. Among them, ELISA has widely been used with the advantages of being simple to operate and highly selective while providing reproducible results. Thus, it has been considered as a gold standard in detecting pesticide residues. However, the LOD for triazophos using ELISA was approximately 0.1 ng/mL and does not reach the required residual levels in some actual measurement cases. Hence, more sensitive and specific methods for detecting triazophos residue are urgently needed.

In recent years, nanomaterials have been found to exhibit excellent characteristics in immunoassays, owing to their small size, high surface area, and quantum size effect, (Devi et al., 2015; Peterson et al., 2015). AuNPs are the most interesting metal nanoparticles and have been widely used in various studies (Lee et al., 2015; Sztandera et al., 2019). AuNPs

present fascinating performance due to their properties (Marie-Christine and Didier, 2004). AuNPs are of interest as ideal carriers and able to bind strongly with different biomolecules, such as biomacromolecules (proteins and DNA), polynucleotides, thiol compounds, and amino acids (Lee et al., 2010; Lori et al., 2012). Particular interest in bio -barcodes (combined with AuNPs and immunoassays) has been emerged because of their powerful amplification ability with displayed sensitivity comparable to that of PCR for detection of biomarkers in the absence of enzyme amplification (Jwa-Min et al., 2004). In this context, Chen et al. (2020) developed a highly sensitive and selective fluorescence detection of ochratoxin A based on a bio-barcode immunoassay and catalytic hairpin assembly signal amplification. On the other hand, Cui et al. (2019) designed a methodology for sensitive determination of triazophos using droplet digital PCR combined with bio-barcode immunoassay. Without the need to use the time-consuming PCR amplification, this new aptamer-based bio-barcode assay can be used for detection and screening the anti-cancer drugs (Loo et al., 2017). Furthermore, in 2010, Han's group initially developed a novel multiplex immunoassay—the oligonucleotide-linked immunoassay (OLISA)—that was based on a detection antibody conjugated with DNA (Ki-Cheol et al., 2010). This facile analysis system presented reproducible detection results for three common cancer markers and exhibited a similar LOD to ELISA with a microwell plate-based platform. All these studies demonstrated that the bio-barcode AuNPs combination could be a promising strategy in immunoassays. Multiple studies were focused on bio-barcode amplification system for detection of various biomacromolecules via sandwich assays. Notably, sandwich assay is not applicable for detection of pesticides and other small molecules, because they contain only one antibody binding site.

Herein, we developed a novel and facile immunoassay to detect triazophos based on AuNPs and a bio-barcode amplification strategy. Owing to the high surface effect, this method was designed based on the AuNPs and labelled with a large amount of single-stranded DNA (ssDNA) and mAbs, instead of protein. The ssDNA-AuNPs-mAbs are acted as a carrier for signal amplification. The complementary RNA probes are modified with a pair of fluorophore/quenchers at each end. RNase H is an endoribonuclease that hydrolyzes the phosphodiester bonds of RNA, which hybridized to DNA. The fluorescence emission was produced after separation of fluorophore from quencher on the RNA. Remarkably, this enzyme can only disintegrate the RNA in DNA-RNA duplexes, and does not digest single or double-stranded DNA. The DNA-RNA hybridization, therefore, is based on repeated cycles that amplify the detection signal. Because the reaction conditions are relatively strict, adequate fluorescence for a good signal to noise ratio was only achieved under dark conditions. Therefore, the last step of our experimental protocol was conducted in the dark to properly reduce back ground and the experimental error. The high surface effect of AuNPs and iterative cycles of the hybridization could enhance the detection signal. Clearly, the specific recognition and hydrolysis of RNase improves the accuracy of the method. Hence, this amplification strategy provides a new perspective for detecting trace amounts of chemicals.

2. Materials and methods

2.1 Materials and reagents

Polyethylene glycol 20000 (PEG 20000), Tris-EDTA (TE) buffer (pH 7.4), ovalbumin (OVA), tris (2-carboxyethyl) phosphine (TCEP), dithiothreitol (DTT), and bovine serum albumin (BSA) were purchased from Sigma-Aldrich (St. Louis, MO, USA). The triazophos haptens (illustrated in Supplementary material) and monoclonal antibodies (mAbs) (4.53 mg/mL) were donated by the Institute of Pesticide and Environmental Toxicology (Zhejiang University, Zhejiang, China). Standards for triazophos (98%) and structural analogues (>95%) were procured from Dr. Ehrenstorfer GmbH (Augsburg, Germany). RNase H was purchased from Takara (Kusatsu, Japan). All oligonucleotides were generated by the Shanghai Sangon Biotechnology Co., Ltd. (Shanghai, China).

2.2 ssDNA-AuNPs-mAbs complex preparation

The preparation of AuNPs probe complex was carried out based on a previously published protocol with some modifications (Zhang et al., 2017). First, 5'-thiolated ssDNA (1 OD) (5'-AAAAAAAAAAAGCGTTGTAG -3')was activated with TE buffer and 20 mmol/L TCEP solution at room temperature for 3 h under mild agitation. After filtering through a 0.22 μm polyethersulfone (PES) membrane, the pH of a 1 mL 13 nm-AuNPs solution was adjusted to 9.0 with 0.2 mol/L K2CO3. Afterward, 4 μL of mAb for triazophos was added to AuNPs solution and incubated for 1 h at room temperature. The mAbs-modified AuNPs solution was mixed into thiolated ssDNA and completely reacted for at least 16 h at 4 °C. Subsequently, the ssDNA-AuNPs-mAbs complex solution was stabilized by serially adding 30% PEG 20000 and 0.1 mol/L phosphate buffered saline (PBS) (pH 7.0) for 8 h, and the solution was blocked on the bare surfaces by adding 10% BSA. Finally, the mixture was centrifuged for 15 min at 6708 ×g to remove unbound ssDNA and mAbs. The supernatant was removed, and the precipitate was resuspended in 200 μL of 0.01 mol/L PBS (pH 7.4) containing 1% BSA and 1% PEG 20000.

2.3 Detection of triazophos using a bio-barcode amplification strategy

The detection procedure for triazophos was as follows: A volume of 100 μL (per well) of OVA-triazophos hapten (3.78 mg/L, OVA- hapten conjugates was prepared as described by (Gui et al., 2006) was added into a 96-MicroWell™ Black Plate after being serially diluted with 0.01 mol/L PBS and then incubated at 4 °C overnight. Subsequently, the coated plate was rinsed with PBST (0.01 mol/L PBS containing 0.05% Tween-20, 300 μL×3) and blocked by blocking buffer (300 μL, 1% BSA in 0.01 mol/L PBS) at 37 °C for 1 h. The plate was then washed three times with PBST before triazophos standard solution (50 μL, diluted in 5% methanol-PBS or sample extract) and ssDNA-AuNPs-mAbs complex (50 μL, diluted in 0.01 mol/L PBS) were separately added, followed by incubation for 1 h at 37 °C. The unbound triazophos and ssDNA-AuNPs-mAbs complex were removed through washing three times with PBST, and the coated ssDNA-AuNPs-mAbs complex was used for the next reaction step. Afterward, a 100 μL of RNase H reaction solution (Tris-HCl buffer (pH 7.5) consisting of 10 mmol/L DTT, 6 mmol/L $MgCl_2$, 0.1 μmol/L RNA probe (Cy5-CUACAACGCU-BHQ1)), and 6 U of RNase H was added to the system to generate a fluorescence signal (Seo et al., 2015). After reaction for 90 min at 37 °C, the fluorescence

intensity changes (Ex 640 nm/Em 675 nm) were immediately measured by an Infinite M200 PRO Microplate reader (TECAN, Männedorf, Switzerland).

2.4 Characterization of reaction system

Herein, the detection procedure can be divided into immunochemical and detection reaction. The optimization of the immunochemical reaction is quite critical to improve both the sensitivity and accuracy of the method. Additionally, RNase H is an endoribonuclease that specifically hydrolyzes the phosphodiester bonds of RNA, which is hybridized to DNA (Schultz and Champoux, 2008). Only through the hybridization of DNA-RNA and the specific hydrolysis of RNase H, the detection signal is generated after separation of fluorophore from quencher on the DNA-RNA duplex. The accuracy and sensitivity of method are directly dependent on fluorescence lifetime and intensity. To maximize the fluorescence signal, the reaction conditions (immunochemical reaction and detection reaction) were further optimized during the experimental protocol.

2.5 Analysis of triazophos in food samples

Sample preparation was carried out according to the quick, easy, cheap, effective, rugged, and safe (QuEChERS) method with some modifications (Anastassiades et al., 2003). The tested samples, apple, turnip, cabbage, and rice, were procured from local markets (Beijing, China). All samples were determined to be free of triazophos by LC-MS/MS. Briefly, 10 mL filtered surface water and 10 g chopped samples (for rice, 5 g + 5 mL water) were spiked with three concentrations of triazophos (5, 10, and 50 μg/kg) and allowed to stand for 30 min. Then, 10 mL acetonitrile was added and the mixture was homogenized for 1 min. Following the addition of 1 g of NaCl and 4 g of $MgSO_4$, the mixture was centrifuged for 5 min at 2795 ×g to remove water and salt. Afterward, 3 mL supernatant was transferred into centrifuge tubes containing 150 mg primary-secondary amine (PSA), 150 mg trimethoxy(octadecyl)silane (C_{18}), and 450 mg $MgSO_4$ and once again centrifuged for 5 min at 2795 ×g. Finally, the extractant was filtered through a 0.22 μm membrane filter for further detection. Half of the supernatant was used for residue analysis using LC-MS/MS (as shown in Supplementary material) (Zhang et al., 2017), whereas the second half was concentrated under a stream of nitrogen and then tested using the developed method after being diluted 20 times in 5% methanol-PBS.

2.6 Statistical analysis

The entire study was repeated at least three times. Data were analysed using Origin 8.5 for windows.

$$I=\frac{F_{max}-F_X}{F_X-F_0}\times 100\,\%$$

where “I” represents the fluorescence intensity inhibition; “F_{max}” is the maximum fluorescence intensity (the reaction system without adding triazophos); “F_x” is the fluorescence intensity related to triazophos concentration; “F_0” is the fluorescence intensity in blank wells.

3. Results and discussion

3.1 Characterization of AuNPs probe

Excellent dispersion and uniform size of AuNPs can be effectively modified with sufficient ssDNA and mAbs, which improves the accuracy and sensitivity of the reaction system. Therefore, we have characterized the AuNPs and ssDNA-AuNPs-mAbs by transmission electron microscopy (TEM). As shown in TEM image, the AuNPs (Fig. 1A) and ssDNA-AuNPs-mAbs (Fig. 1B) displayed uniform size and good dispersibility. Additionally, both solutions were transparent and no aggregations have been observed in photographs. The ssDNA-AuNPs-mAbs play a crucial role in signal amplifying assay for triazophos detection. So, the successful modification of AuNPs was used as a basis for this method. It was reported that functionalized AuNPs could exhibit a visible colour change associated with a transition from the dispersion to an aggregated state and have excellent selectivity and sensitivity for a target substance (Li et al., 2010). Preliminarily, we found that AuNPs are covered by mAbs and ssDNA through comparing the two photos. This is because the colour of ssDNA-AuNPs-mAbs solution had changed from red to amaranth. To demonstrate that the AuNPs were successfully synthesized with mAbs and ssDNA, we characterized those compounds using UV-Vis spectroscopy. This behaviour was also apparent from the UV-Vis absorption spectra of AuNPs and ssDNA-AuNPs-mAbs (Fig. 1C). The ssDNA-AuNPs-mAbs exhibited an absorption peak at 528 nm, and the maximum absorbance wavelength shifted from 520 nm (AuNPs) to 528 nm. There have been some reports that have chosen this simple and rapid method to characterize compounds (Ma et al., 2018; Tae-Il et al., 2011).

3.2 Optimization of the immunochemical reaction

The pH and buffer concentration can substantially affect the performance of the immunochemical reaction. Herein, phosphate-buffered saline solution was selected to explore the effects of pH and concentration on the immunochemical reaction. As complied in Table S1, 0.01 mol/L PBS solution with pH 7.4 exhibited better performance; the sensitivity of method was found to be 1.89 and $Fmax/IC_{50}$ reached the maximum value. Therefore, 0.01 mol/L PBS buffer with pH 7.4 was chosen for the immunochemical reaction buffer and used throughout the experimental work.

A study conducted by Yan et al(2014) demonstrated that methanol concentration could influence the dissolution of pesticides and may impact the specific reaction between mAbs and haptens. Therefore, the appropriate addition of methanol is needed to improve the sensitivity of the assay system. After optimizing the immunoreagent dilutions of OVA-hapten and ssDNA-AuNPs-mAbs (Supplementary Table 2), we have investigated the effect of methanol concentration on the fluorescence signal. Fig. 2 clearly shows that the fluorescence intensity gradually increased following the addition of various concentrations of methanol to 0.01 mol/L PBS. Moreover, the higher the ratio of F_{max}/IC_{50} (IC_{50}, the concentration that produced 50% inhibition of the maximum fluorescence intensity) the higher the sensitivity. The value dramatically increased and reached the maximum when the methanol concentration reached 5% in 0.01 mol/L. Thus, 5% methanol-PBS (0.01 mol/L) was selected as the optimal solution for further experimental work.

3.3 Optimization of detection reaction

As a reducing agent, dithiothreitol (DTT) prevents the oxidation of sulfhydryl groups and hence maintains the activity of proteins (Banik et al., 2015). Optimal DTT concentration would maximize the RNase H activity leading to improved immunoassay with great performance. The influence of DTT concentration on fluorescence intensity was therefore examined. As shown in Fig. 3, the fluorescence intensity exhibited substantial enhancement after the addition of DTT. The intensity gradually increased as the DTT concentration increased and reached a maximum value at 10 mmol/L. It has to be noted that excess DTT can break disulfide bonds and destroy the protein structure; our results confirmed this trend as well. The fluorescence intensity decreased as the concentration increases (> 10 mmol/L). Obviously, the addition of 10 mmol/L DTT was appropriate to prevent the sulfhydryl from oxidizing without breaking the disulfide bond and led to improvement of the fluorescence signal.

A variety of factors, such as ionic strength (Park et al., 2007), pH, and temperature, could influence the efficiency of hybridization between the two strands of DNA-RNA. Tris-HCI buffer has become the standard buffer for the storage of nucleic acids and proteins. The effect of ionic strength on the hybridization was investigated using Tris-HCI buffer at different concentration ranging from 20 to 60 mmol/L. As shown in Fig. 4A, fluorescence intensity increased with increases of the buffer concentration until the latter reached 40 mmol/L; the value decreased gradually afterward. Obviously, the ionic strength provided by the 40 mmol/L Tris-HCI buffer was the most effective for hybridization.

The pH may affect not only the hybridization between the two strands of DNA-RNA, but also can substantially influence the enzyme surface charge, catalytic, and binding-ability. The enzyme and the DNA-RNA duplex are denatured at a lower or a higher pH. To maximize the activity of the RNase H and the efficiency of hybridization, the reaction system must be processed under suitable pH conditions. The optimal pH of the reaction solution was determined by measuring the fluorescence intensity at pH values of 3.5, 4.5, 5.5, 6.5, 7.5, 8.5, and 9.5, respectively. Fig. 4B shows the fluorescence intensity increased as pH changed from 3.5 to 7.5, and then decreased thereafter. This result indicates that a pH = 7.5 is the optimal value to maximize the activity of the RNase H and the efficiency of hybridization.

As an important cofactor for many enzymes, metal ion seems to be essential for maintaining an active enzyme conformation and boosting the process of enzymatic reaction. Different enzymes have different metallic cofactors. Mg^{2+} is the cofactor of RNase H and herein we exploit the effect of $MgCl_2$ concentration on the catalytic capacity of RNase H. As shown in Fig. 4C, the fluorescence intensity increased linearly at concentration from 2 to 6 mmol/L, before it continuously decreases as the concentration increases from 6 to 8 mmol/L; reaching the maximum at 6 mmol/L. Obviously, a concentration of 6 mmol/L was selected as the optimal condition.

Similarly, the optimal temperature provides a suitable reaction condition for DNA-RNA hybridization as well as it enhances the RNase H activity and stability. Fig. 5 shows the effect of temperature and reaction time on the fluorescence intensity. As the temperature

increases above the optimum temperature (37 °C) the fluorescence intensity increases, then decreases thereafter. The signal intensity reached the maximum at 37 °C. Furthermore, the fluorescence signal should be observed after adding the RNase H. To investigate the hydrolysis efficiency of RNase H, the effect of the reaction time on the system was investigated. As shown in Fig. 5, the fluorophore can be released gradually and the reaction was completed within 120 min. The change in the fluorescence intensity over the course of hybridization and hydrolysis was slow, and it demonstrates a clear log phase for the first 15 min. As the reaction proceeded, most of fluorophores were dissociated from RNA and the fluorescence intensities increased dramatically between 15–90 min. After 90 min, it was noted that fewer RNA probes were involved in the reaction system; thus the intensity changed slowly. Additionally, our data indicate that fluorophore exhibited remarkable stability within 2 h.

3.4 Bio-barcode amplification system for sensitive detection of triazophos

Under the established optimized assay conditions, the fluorescence intensity as a function of triazophos concentration was evaluated. The results are shown in Fig. 6. The competitive standard curve (y=18.1x+55.2, R^2=0.975) clearly manifested that the fluorescence inhibition was linearly proportional to triazophos concentration (0.01–100 ng/mL). The LOD (the concentration of triazophos that produced 10% inhibition of the maximum fluorescence) was 0.0032 ng/mL and the sensitivity (expressed as IC_{50}) was found to be 0.516 ng/mL. The LOD was substantially lower than CLISA (0.063 ng/mL) (Maojun et al., 2012), BBC-IA (0.024 ng/ mL) (Du et al., 2016), and fluorescence polarization immunoassay (FPIA, 3.62 ng/mL) (Liu Y. et al., 2016). Additionally, this bio-barcode amplification system is one order of magnitude lower than that of the conventional ELISA and met the requirement for detecting pesticides at low-residual level. A comparison of various immunoassays with the current methodology is shown in Table 1.

3.5 Matrix effect

Matrix effect (ME) remains a great challenge for quantitative analysis of pesticide residues in various matrices. Food components, such as sugars, pigments, and organic acids can compromise the sensitivity and selectivity of the analytical method. While matrix effect cannot be eliminated entirely, it can be minimized through suitable dilution times. The matrix effect was assessed by comparing the slope of a calibration curve for standard solutions with that of matrix-matched standard solutions (Liu et al., 2016).

$$\text{Matrix effect (ME \%)} = (1 - \text{slope}_{\text{matrix}}/\text{slope}_{\text{solvent}}) \times 100\,\%$$

If the calculated matrix effects are within the range of −20% and 20%, it can be considered as negligible or insignificant (Guedes et al., 2016). As shown in Table 2, the tested samples (without dilution) showed substantial matrix effects. The matrix effects were then reduced to acceptable levels when the samples were diluted either 10 or 20 fold with 5% methanol-PBS (0.01 mol/L). Therefore, the samples were diluted 20 times.

3.6 The accuracy of the method

To further evaluate the analytical accuracy of the developed bio-barcode immunoassay method, the recovery test was performed, and the results were compared with those obtained from LC-MS/MS. The coefficient of variation (CV) was determined by estimating the recovery rates from blank samples spiked with three fortification concentrations of 5, 10, and 50 μg/kg. The extracts were directly analyzed using LC-MS/MS or concentrated under a stream of nitrogen and then tested by the developed bio-barcode immunoassay after being diluted in 5% methanol-PBS. The average recovery (CV %) of the developed bio-barcode immunoassay and LC-MS/MS was ranged between 73.4% and 116% (CV (%) = 7.04 – 17.4) and 79.4% to 109% (CV = 2.23% - 9.62%), respectively (Table 3). Furthermore, the results were compared on the basis of the correlation coefficients and the linear regression equations. As shown in Fig. 7, the two methods exhibited good correlation coefficients as following: y= 0.991x+0.0218 (R^2=0.984, surface water); y=1.24x+0.630 (R^2=0.982, apple); y=0.809x+2.35 (R^2=0.977, turnip); y=1.07x−0.331 (R^2=0.987, cabbage); and y=0.812x +2.68 (R^2=0.962, rice). In sum, the proposed bio-barcode amplification immunoassay could be a reliable technique for detecting triazophos residues in agriculture products and surface water.

3.7 Analysis of real samples

Randomly selected 30 samples procured from farmer and great markets were monitored and analyzed using the developed method. Although, triazophos residues were not detected in most of the samples; trace amounts were quantified in 3 samples; the levels of which were below the maximum residue limits (apple MRL: 0.01 mg/kg; cabbage MRL: 0.01 mg/kg; rice MRL: 0.1 mg/kg) (Table S3).

4. Conclusions

In the present study, our proposed bio-barcode amplification strategy utilized the hybridization between two strands of DNA-RNA and the RNase medicated specific hydrolysis to improve the sensitivity of the detection system. The quantitative detection of triazophos displayed wide a linear range of 0.01–100 ng/mL with LOD of 0.0032 ng/mL determined under the optimum conditions. The analytical accuracy and reliability of our method have been documented through a recovery test. We, therefore, conclude that the strategy could improve the sensitivity of the reaction system and has great potential for detecting small molecules.

Supplementary Material

Refer to Web version on PubMed Central for supplementary material.

Acknowledgements

This study was financially supported by National Key Research Program of China (No. 2019YFC1604503), NIEHS Superfund Research Program (No. P42 ES04699), and the Central Public-interest Scientific Institution Basal Research Fund for Chinese Academy of Agricultural Sciences (No. 1610072018002).

References

Anastassiades M, Lehotay SJ, Štajnbaher D, & Schenck FJ (2003). Fast and easy multiresidue method employing acetonitrile extraction/partitioning and "dispersive solid-phase extraction" for the determination of pesticide residues in produce. Journal of AOAC International, 86(2), 412–431. [PubMed: 12723926]

Banik SP, Mukherjee S, Pal S, Ghorai S, Majumder R, & Khowala S (2015). Enhancement of extracellular cellobiase activity by reducing agents in the filamentous fungus Termitomyces clypeatus. Biotechnology Letters, 37(1), 175–181. doi:10.1007/s10529-014-1669-0. [PubMed: 25257587]

Bhanot R, & Sangha GK (2018). Effect of in utero and lactational exposure of triazophos on reproductive system functions in male offsprings, Rattus norvegicus. Drug and Chemical Toxicology, 42(5), 519–525. doi:10.1080/01480545.2018.145704. [PubMed: 29681207]

Casado J, Brigden K, Santillo D, & Johnston P (2019). Screening of pesticides and veterinary drugs in small streams in the European Union by liquid chromatography high resolution mass spectrometry. Science of The Total Environment, 670, 1204–1225. doi:10.1016/j.scitotenv.2019.03.207.

Chen R, Sun Y, Huo B, Yuan S, Sun X, Zhang M, Yin N, Fan L, Yao W, Wang J, Han D, Li S, Peng Y, Bai J, Ning B, Liang J, & Gao Z (2020). Highly sensitive detection of ochratoxin A based on bio-barcode immunoassay and catalytic hairpin assembly signal amplification. Talanta, 208, 120405. 10.1016/j.talanta.2019.120405. [PubMed: 31816695]

Cui X, Jin M, Zhang C, Du P, Chen G, Qin G, Jiang Z, Zhang Y, Li M, Liao Y, Wang Y, Cao Z, Yan F, Abd El-Aty AM, & Wang J (2019). Enhancing the Sensitivity of the Bio-barcode Immunoassay for Triazophos Detection Based on Nanoparticles and Droplet Digital Polymerase Chain Reaction. Journal of Agricultural and Food Chemistry, 67(46), 12936–12944. doi:10.1021/acs.jafc.9b05147. [PubMed: 31670953]

Devi RV, Doble M, & Verma RS (2015). Nanomaterials for early detection of cancer biomarker with special emphasis on gold nanoparticles in immunoassays/sensors. Biosensors and Bioelectronics, 68, 688–698. doi:10.1016/j.bios.2015.01.066. [PubMed: 25660660]

Du P, Jin M, Chen G, Zhang C, Jiang Z, Zhang Y, Zou P, She Y, Jin F, & Shao H (2016). A Competitive Bio-Barcode Amplification Immunoassay for Small Molecules Based on Nanoparticles. Scientific Reports, 6, 38114. doi:10.1038/srep3811. [PubMed: 27924952]

Guedes JAC, Silva R. d. O, Lima CG, Milhome MAL, & do Nascimento RF (2016). Matrix effect in guava multiresidue analysis by QuEChERS method and gas chromatography coupled to quadrupole mass spectrometry. Food Chemistry, 199, 380–386. 10.1016/j.foodchem.2015.12.007. [PubMed: 26775985]

Gui WJ, Jin RY, Chen ZL, Cheng JL, & Zhu GN (2006). Hapten synthesis for enzyme-linked immunoassay of the insecticide triazophos. Analytical Biochemistry, 357(1), 9–14. 10.1016/j.ab.2006.07.023. [PubMed: 16920057]

Guo Y, Liu R, Liu Y, Xiang D, Liu Y, Gui W, Li M, & Zhu G (2018). A non-competitive surface plasmon resonance immunosensor for rapid detection of triazophos residue in environmental and agricultural samples. Science of The Total Environment, 613–614,783–791. doi:10.1016/j.scitotenv.2017.09.157.

Hayward DG, Wong JW, & Park HY (2015). Determinations for Pesticides on Black, Green, Oolong, and White Teas by Gas Chromatography Triple-Quadrupole Mass Spectrometry. Journal of Agricultural and Food Chemistry, 63(37), 8116–8124. doi:10.1021/acs.jafc.5b02860. [PubMed: 26209005]

Jwa-Min N, Stoeva SI, & Mirkin CA (2004). Bio-bar-code-based DNA detection with PCR-like sensitivity. Journal of the American Chemical Society, 126(19), 5932–5933. doi:10.1021/ja049384+. [PubMed: 15137735]

Ki-Cheol H, Dae-Ro A, & Eun Gyeong Y (2010). An approach to multiplexing an immunosorbent assay with antibody-oligonucleotide conjugates. Bioconjugate Chemistry, 21(12), 2190–2196. doi:10.1021/bc100147a. [PubMed: 21105685]

Lee HU, Shin HY, Lee JY, Song YS, Park C, & Kim SW (2010). Quantitative Detection of Glyphosate by Simultaneous Analysis of UV Spectroscopy and Fluorescence Using DNA-Labeled Gold

Nanoparticles. Journal of Agricultural and Food Chemistry, 58(23), 12096–12100. doi:10.1021/jf102784t. [PubMed: 21047070]

Lee J, Ahmed SR, Oh S, Kim J, Suzuki T, Parmar K, Park SS, Lee J, & Park EY (2015). A plasmon-assisted fluoro-immunoassay using gold nanoparticle-decorated carbon nanotubes for monitoring the influenza virus. Biosensors and Bioelectronics, 64, 311–317. doi:10.1016/j.bios.2014.09.021. [PubMed: 25240957]

Li M, Hua X, Ma M, Liu J, Zhou L, & Wang M (2014). Detecting clothianidin residues in environmental and agricultural samples using rapid, sensitive enzyme-linked immunosorbent assay and gold immunochromatographic assay. Science of The Total Environment, 499, 1–6. doi:10.1016/j.scitotenv.2014.08.029.

Li Y, Wu P, Xu H, Zhang H, & Zhong X (2010). Anti-aggregation of gold nanoparticle-based colorimetric sensor for glutathione with excellent selectivity and sensitivity. Analyst, 136(1), 196–200. [PubMed: 20931106]

Liu B, Gong H, Wang Y, Zhang X, Li P, Qiu Y, Wang L, Hua X, Guo Y, & Wang M (2018). A gold immunochromatographic assay for simultaneous detection of parathion and triazophos in agricultural products. Analytical Methods, 10, 422–428. doi:10.1039/C7AY02481.

Liu Y, Liu R, Boroduleva A, Eremin S, Guo Y, & Zhu G (2016). A highly specific and sensitive fluorescence polarization immunoassay for the rapid detection of triazophos residue in agricultural products. Analytical Methods, 8(36), 6636–6644. doi:10.1039/C6AY00908E.

Loo JF-C, Yang C, Tsang HL, Lau PM, Yong K-T, Ho HP, & Kong SK (2017). An Aptamer Bio-barCode (ABC) assay using SPR, RNase H, and probes with RNA and gold-nanorods for anti-cancer drug screening. Analyst, 142(19), 3579–3587. doi:10.1039/C7AN01026E. [PubMed: 28852760]

Lori R, Aruna Jyothi K, & Arunachalam J (2012). Highly stable, protein capped gold nanoparticles as effective drug delivery vehicles for amino-glycosidic antibiotics. Materials Science and Engineering: C, 32(6), 1571–1577. doi:10.1016/j.msec.2012.04.044. [PubMed: 24364962]

Lu H, Quan S, & Xu S (2017). Highly Sensitive Ratiometric Fluorescent Sensor for Trinitrotoluene Based on the Inner Filter Effect between Gold Nanoparticles and Fluorescent Nanoparticles. Journal of Agricultural and Food Chemistry, 65(44), 9807–9814. doi:10.1021/acs.jafc.7b03986. [PubMed: 29068213]

Ma S, He J, Guo M, Sun X, Zheng M, & Wang Y (2018). Ultrasensitive colorimetric detection of triazophos based on the aggregation of silver nanoparticles. Colloids and Surfaces A: Physicochemical and Engineering Aspects, 538, 343–349. doi:10.1016/j.colsurfa.2017.11.030.

Maojun J, Hua S, Fen J, Wenjun G, Xiaomei S, Jing W, & Guonian Z (2012). Enhanced competitive chemiluminescent enzyme immunoassay for the trace detection of insecticide triazophos. Journal of Food Science, 77(5), T99–T104. doi:10.1111/j.1750-3841.2012.02659.x. [PubMed: 22490114]

Marie-Christine D, & Didier A (2004). Gold nanoparticles: assembly, supramolecular chemistry, quantum-size-related properties, and applications toward biology, catalysis, and nanotechnology. Chemical Reviews, 35(16), 293–346. doi:10.1021/cr030698+.

Park H, Germini A, Sforza S, Corradini R, Marchelli R, & Knoll W (2007). Effect of ionic strength on PNA-DNA hybridization on surfaces and in solution. Biointerphases, 2(2), 80–88. doi:10.1116/1.2746871. [PubMed: 20408640]

Peterson RD, Chen W, Cunningham BT, & Andrade JE (2015). Enhanced sandwich immunoassay using antibody-functionalized magnetic iron-oxide nanoparticles for extraction and detection of soluble transferrin receptor on a photonic crystal biosensor. Biosensors and Bioelectronics, 74, 815–822. doi:10.1016/j.bios.2015.07.050. [PubMed: 26232676]

Rai S, Singh AK, Srivastava A, Yadav S, Siddiqui MH, & Mudiam MKR (2016). Comparative Evaluation of QuEChERS Method Coupled to DLLME Extraction for the Analysis of Multiresidue Pesticides in Vegetables and Fruits by Gas Chromatography-Mass Spectrometry. Food Analytical Methods, 9(9), 2656–2669. doi:10.1007/s12161-016-0445-.

Schultz SJ, & Champoux JJ (2008). RNase H activity: Structure, specificity, and function in reverse transcription. Virus Research, 134(1), 86–103. doi:10.1016/j.virusres.2007.12.007. [PubMed: 18261820]

Seo SH, Lee YR, Jeon JH, Hwang YR, Park PG, Ahn DR, Han KC, Rhie GE, & Hong KJ (2015). Highly sensitive detection of a bio-threat pathogen by gold nanoparticle-based oligonucleotide-linked immunosorbent assay. Biosensors and Bioelectronics, 64, 69–73. doi:10.1016/j.bios.2014.08.038. [PubMed: 25194798]

Singh S, Tiwari RK, & Pandey RS (2018). Evaluation of acute toxicity of and imidacloprid. Analytical Methods, 4(12), 4053. doi:10.1016/j.scitotenv.2014.08.029.

Zhang C, Du P, Jiang Z, Jin M, Chen G, Cao X,, Cui X, Zhang Y, Li R, & Abd El-Aty AM. (2017). A simple and sensitive competitive bio-barcode immunoassay for triazophos based on multi-modified gold nanoparticles and fluorescent signal amplification. Analytica Chimica Acta, 999, 123–131. doi:10.1016/j.aca.2017.10.032. [PubMed: 29254562]

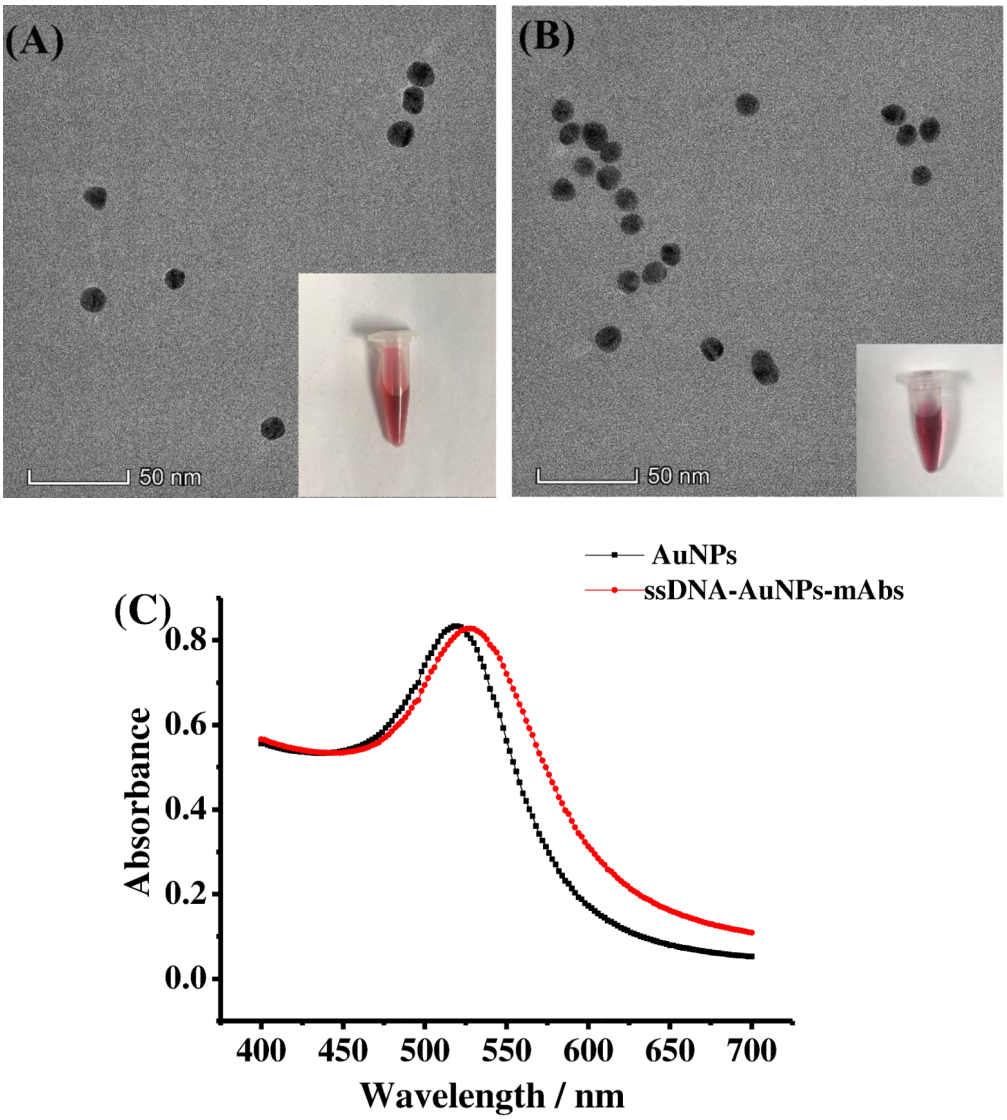

Fig. 1.

Characterization of AuNP and AuNPs modified with mAbs and ssDNA. (A) Photograph and TEM analysis of AuNPs, (B) Photograph and TEM analysis of ssDNA-AuNPs- mAbs, and (C) UV-Vis spectroscopy of AuNPs (black line) and ssDNA-AuNPs-mAbs (redline).

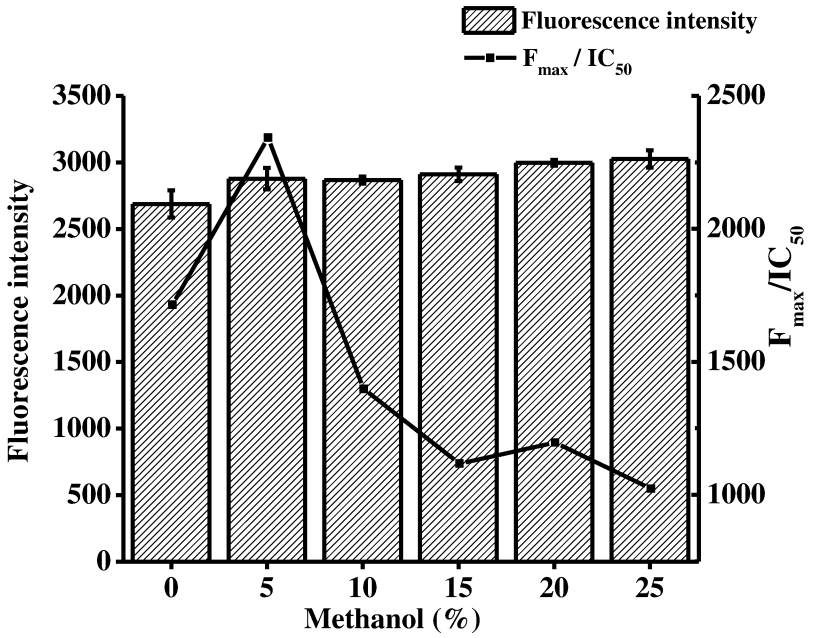

Fig. 2.
The effect of methanol concentration on fluorescence intensity and F_{max}/IC_{50}.

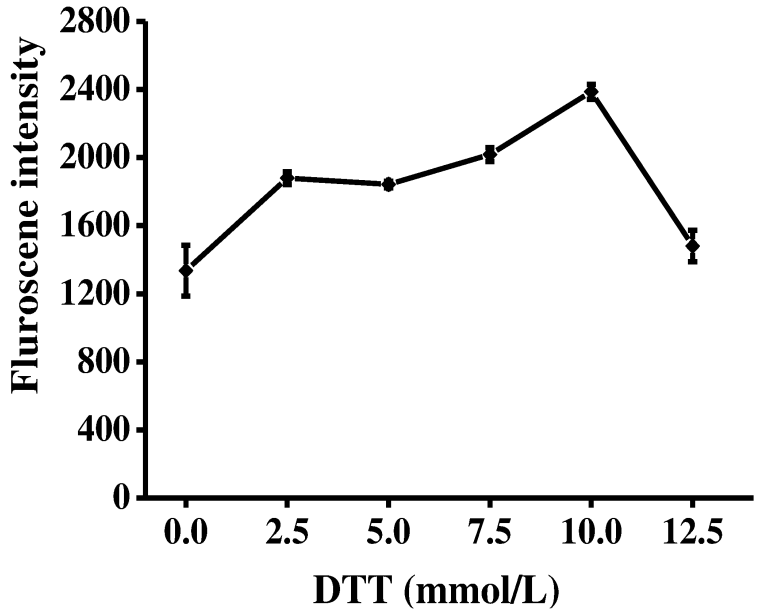

Fig. 3.
The effect of dithiothreitol (DTT) concentration on fluorescence intensity.

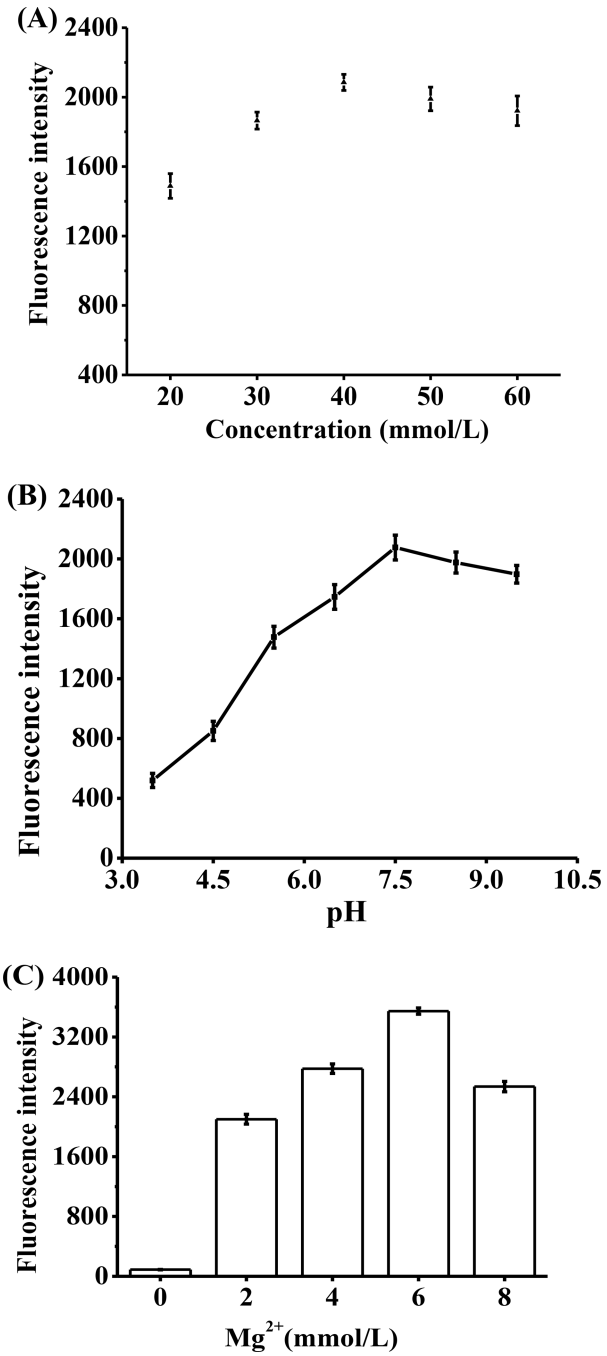

Fig. 4.

Effect of Tris-HCI buffer (A), pH (B), and Mg^{2+} concentration (C) on fluorescence intensity at 37 °C. Error bars were based on three replicate experiments.

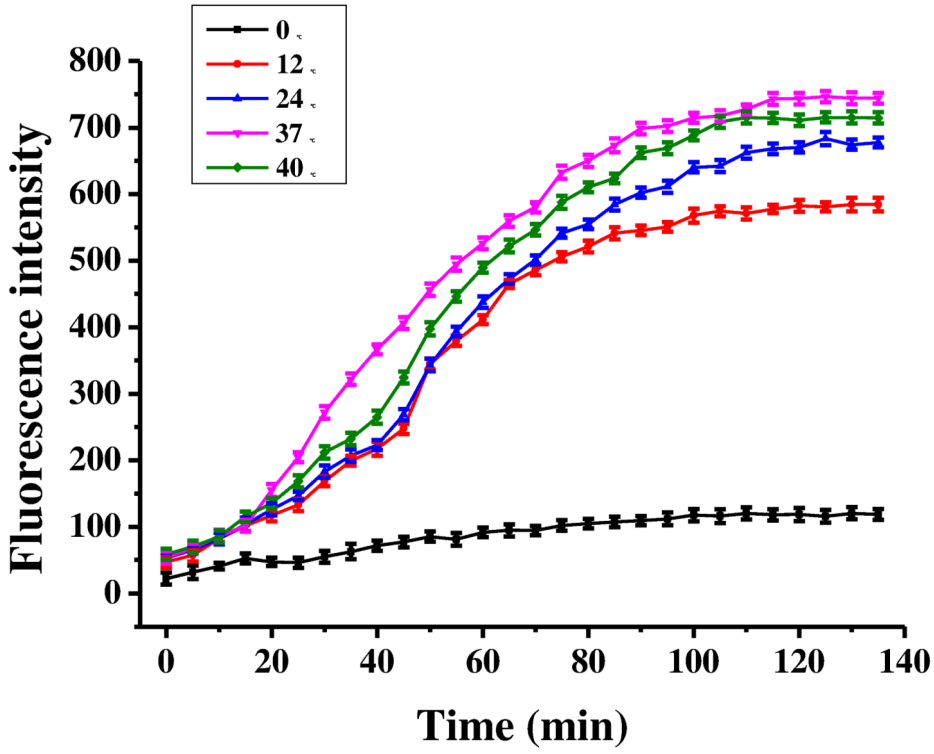

Fig. 5.

Effect of temperature and reaction time on the fluorescence intensity. The fluorescence intensity of the amplification system was measured periodically every 5 min.

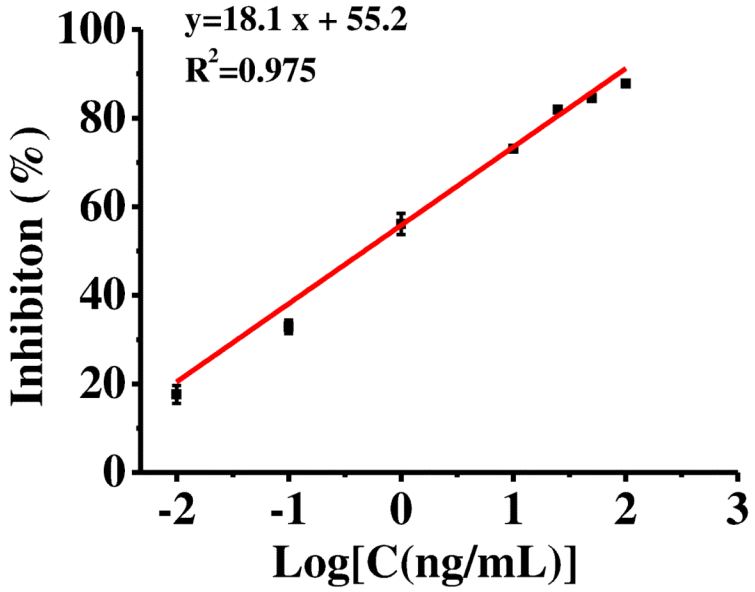

Fig. 6.

The standard curve of the proposed bio-barcode amplification immunoassay method at a wide linear range of 0.01 and 100 ng/mL.

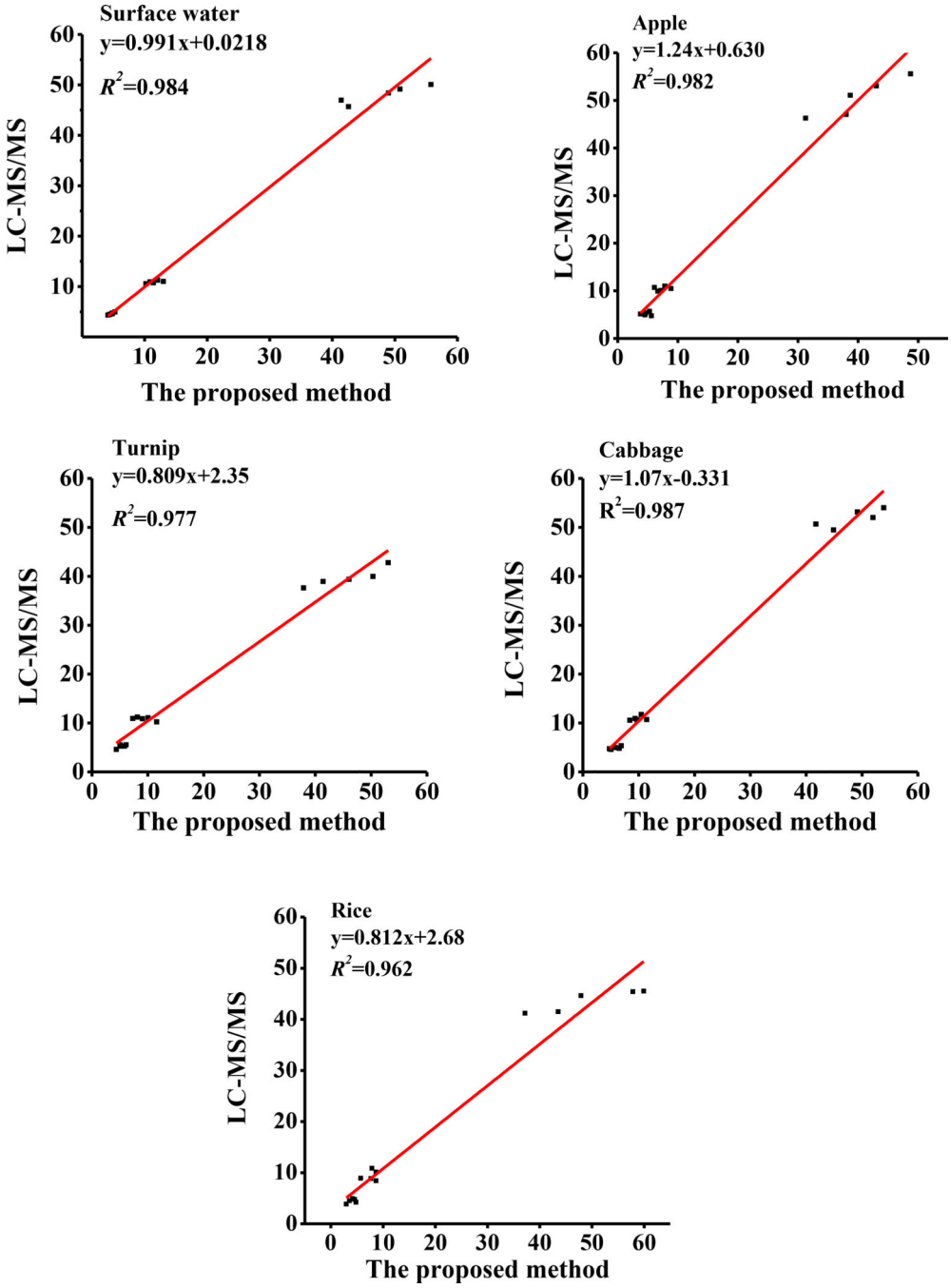

Fig. 7.

Correlation between the proposed method and LC-MS/MS for detection of triazophos residue in foodstuffs and surface water.

Table 1.

Comparison of various immunoassays.

Method	IC_{50} (ng/mL)	LOD (ng/mL)	Linear range (ng/mL)	Samples
FPIA	3.62	2.9×10^{-2}	1.25–10.48	water, rice, cabbage, apple
CLEIA	0.87	6.30×10^{-2}	0.04–5	lettuce, carrot, apple, water, soil
BBC-IA	NA	2.00×10^{-2}	0.04–10	apple, orange, cabbage, rice
This work	0.514	3.20×10^{-3}	0.01–100	water, apple, turnip, rice, cabbage

FPIA: Fluorescence polarization immunoassay

CLEIA: Chemiluminescence enzyme immunoassay

BBC-IA: bio-barcode immunoassay

NA: Not available

Table 2.

Assessing the matrix effects (%) across a dilution range in samples (n=3).

Dilution	Apple	Cabbage	Rice
1:1	31.2	33.7	31.0
1:10	18.8	14.7	14.2
1:20	7.57	−1.96	6.21

Table 3.

Recovery and the CV of the proposed bio-barcode immunoassay and LC-MS/MS (n=5).

Samples	Spiked concentration (μg/kg)	Bio-barcode immunoassay		LC-MS/MS	
		Recovery (%)	CV (%)	Recovery (%)	CV (%)
Surface water	5	94.2	7.33	92.6	4.66
	10	115	7.04	109	2.23
	50	95.8	9.39	96.2	3.26
Apple	5	95.6	13.2	104	6.22
	10	73.4	13.0	104	3.71
	50	80.0	14.5	101	6.98
Turnip	5	106	11.5	105	6.70
	10	92.2	16.2	109	3.02
	50	91.6	12.2	79.4	4.29
Cabbage	5	116	14.0	98.0	5.13
	10	98.7	10.4	109	3.87
	50	96.6	9.24	104	3.17
Rice	5	80.2	16.9	89.0	8.80
	10	76.9	14.0	94.4	9.62
	50	98.6	17.4	87.4	4.35